

Finite-size effects on the dynamic susceptibility of CoPhOMe single-chain molecular magnets in presence of a static magnetic field

M. G. Pini,¹ A. Rettori,² L. Bogani,³ A. Lascialfari,^{4,5} M. Mariani,⁴ A. Caneschi,⁶ and R. Sessoli⁶

¹*Istituto dei Sistemi Complessi, Consiglio Nazionale delle Ricerche, I-50019 Sesto Fiorentino, Firenze, Italy*

²*Dipartimento di Fisica and CNISM, Università di Firenze, I-50019 Sesto Fiorentino, Firenze, Italy*

³*1. Physikalisches Institut, Universität Stuttgart, D-70550 Stuttgart, Germany*

⁴*Dipartimento di Fisica "A. Volta," Università di Pavia, I-27100 Pavia, Italy*

⁵*Dipartimento di Scienze Molecolari Applicate ai Biosistemi, Università di Milano, I-20134 Milano, Italy*

⁶*Dipartimento di Chimica and INSTM, Università di Firenze, I-50019 Sesto Fiorentino, Firenze, Italy*

(Received 4 May 2011; revised manuscript received 30 June 2011; published 26 September 2011)

The static and dynamic properties of the single-chain molecular magnet $\text{Co}(\text{hfac})_2\text{NITPhOMe}$ (CoPhOMe) (hfac = hexafluoroacetylacetonate, NITPhOMe = 4'-methoxy-phenyl-4,4,5,5-tetramethylimidazoline-1-oxyl-3-oxide) are investigated in the framework of the Ising model with Glauber dynamics, in order to take into account both the effect of an applied magnetic field and a finite size of the chains. For static fields of moderate intensity and short chain lengths, the approximation of a monoexponential decay of the magnetization fluctuations is found to be valid at low temperatures; for strong fields and long chains, a multiexponential decay should rather be assumed. The effect of an oscillating magnetic field, with intensity much smaller than that of the static one, is included in the theory in order to obtain the dynamic susceptibility $\chi(\omega)$. We find that, for an open chain with N spins, $\chi(\omega)$ can be written as a weighted sum of N frequency contributions, with a sum rule relating the frequency weights to the static susceptibility of the chain. Very good agreement is found between the theoretical dynamic susceptibility and the ac susceptibility measured in moderate static fields ($H_{\text{dc}} \leq 2$ kOe), where the approximation of a single dominating frequency for each segment length turns out to be valid. For static fields in this range, data for the relaxation time, τ versus H_{dc} , of the magnetization of CoPhOMe at low temperature are also qualitatively reproduced by theory, provided that finite-size effects are included.

DOI: [10.1103/PhysRevB.84.094444](https://doi.org/10.1103/PhysRevB.84.094444)

PACS number(s): 75.50.Xx, 75.40.Gb, 75.10.Hk, 76.20.+q

I. INTRODUCTION

It is commonly admitted that the plain Ising Hamiltonian does not contain any dynamics.¹ In fact, when considering a system of Ising spins σ_i localized at the sites i of a lattice,

$$\mathcal{H} = -J_I \sum_{ij} \sigma_i \sigma_j, \quad \sigma_i = \pm 1, \quad (1)$$

the physically interesting quantities, the σ_i 's, commute with \mathcal{H} . However, for a system in contact with a heat bath, a stochastic dynamics can be introduced by means of a master equation which assumes Markovian processes inducing random flips between different states. One of the few cases in which the problem can be solved analytically is for a one-dimensional lattice, with zero external magnetic field, and an opportune choice of the transition probability, as devised by Glauber² some decades ago. He calculated the dynamic susceptibility within a linear response framework, and found that the uniform magnetization decays exponentially, with a relaxation time given by an Arrhenius law

$$\tau(T) = \tau_0 e^{4J_I/k_B T}, \quad (2)$$

where $1/\tau_0$ is the relaxation rate for an isolated spin. Considering that, at low temperatures, the correlation length for model (1) in one dimension is given by $\xi \propto e^{2J_I/k_B T}$,³ the dynamic critical exponent results in $z = 2$.⁴ Glauber's dynamics has been applied ever since in very different areas, comprising structural phase transitions,⁵ neural networks,⁶ chemical reactivity,⁷ and even biosocioeconomics.^{8,9}

The recent discovery of single-chain magnets¹⁰ (SCMs) spurred renewed interest in Glauber's dynamics in magnetic nanomaterials. Such systems show magnetic hysteresis without the onset of three-dimensional magnetic ordering. At very low temperatures, the relaxation of the magnetization is so slow that other very interesting dynamic phenomena have also been observed with unprecedented clarity, including collective reversal¹¹ and quantum tunneling.¹² As a result, after the discovery of the archetypal SCM [$\text{Co}(\text{hfac})_2\text{NITPhOMe}$] (hereafter denoted CoPhOMe),¹⁰ the number of SCM compounds has been rapidly increasing.¹³⁻²⁰

The strong exchange interaction and one-dimensional character of CoPhOMe (Ref. 10) make it the ideal system in which to observe the long-predicted² slow relaxation of the magnetization. In CoPhOMe, owing to the very high value of the exchange constant ($J_I/k_B = 80$ K), the correlation length ξ is huge, at low temperatures, in a zero magnetic field. Consequently, the unavoidable presence of even a small density of defects causes the chain to break into finite segments whose average length \bar{L} can be much smaller than the correlation length ξ . In such a finite-size regime, $\bar{L} \ll \xi$, the dynamics of the system in zero field is modified^{21,22} with respect to Glauber's analysis of the infinite chain.² In particular the relaxation time, measured in CoPhOMe using ac susceptibility and superconducting quantum interference device (SQUID) magnetization decay techniques, was found to follow an Arrhenius law with a halved energy barrier²³⁻²⁵

$$\tau(T) = \tau_0(\bar{L}) e^{2J_I/k_B T}, \quad (3)$$

in agreement with theoretical predictions of finite-size effects.^{21,22}

These effects were systematically investigated in CoPhOMe by introducing nonmagnetic impurities.²⁶ For nominally pure and impure samples, the complex susceptibility $\chi(\omega) = \chi'(\omega) + i\chi''(\omega)$ was measured in the presence of a moderate static magnetic field ($H_{dc} = 2$ kOe) and of a much smaller ac field oscillating at frequency ω . A two-peaked structure was found in $\chi'(\omega)$ as a function of temperature: the low-temperature peak is frequency dependent, while the high-temperature one is not. On the basis of transfer matrix calculations for the static susceptibility of the doped chain, the low-temperature peak was attributed to finite-size effects.²⁶ Anyway, the frequency dependence of the peak for $\chi'(\omega)$ and $\chi''(\omega) \neq 0$ remains unexplained. Static and dynamic susceptibilities with a similar behavior have also been observed in different cobalt-organic single-chain magnets,²⁷ in the presence of a moderate static magnetic field ($H_{dc} = 0.5$ kOe) and of lattice imperfections. The explanation of such features is thus becoming more pressing, as it can constitute an important tool for the analysis of the properties of a whole class of magnetic systems.

In systems with a very large correlation length, like the one-dimensional Ising model at low temperatures, the introduction of an external magnetic field can have dramatic consequences. A static field H_{dc} strongly depresses the correlation length ξ ,³ and this fact, in turn, should also strongly affect the dynamic susceptibility. The Glauber dynamics of the infinite Ising chain model in an external magnetic field was studied some years ago in order to describe the kinetics of the helix-coil transition in biopolymers.²⁸ For single-chain magnets, a theoretical and experimental study was recently performed by Coulon *et al.*²⁹ focusing on the relaxation time of the magnetization fluctuations. In addition to a static magnetic field, their theoretical analysis²⁹ considered finite-size effects, relevant in SCMs. A local-equilibrium approximation was adopted²⁹ in order to truncate the infinite hierarchy of kinetic equations for finite open Ising chains in $H_{dc} \neq 0$. The main advantages of this approximation, first proposed by Huang³⁰ for infinite chains, are that (i) it provides the exact steady-state solution,³⁰ in contrast with the mean-field approximation; (ii) it is valid for any value of the applied field, in contrast with perturbation methods.²

In this work, we develop the theoretical framework necessary to analyze the ac susceptibility measurements of single-chain magnets in the presence of a static magnetic field H_{dc} . We include in the theory²⁹ the effect of an oscillating magnetic field with intensity much smaller than that of the static one, using a linear response framework. With these theoretical tools, we can account for the dynamic behavior of CoPhOMe and other single-chain magnets. We directly compare the calculated frequency-dependent magnetic susceptibility (representing the response function of the system² to an oscillating magnetic field) with previous^{24,26} and additional experimental measurements of the ac susceptibility in the presence of a nonzero static magnetic field H_{dc} . In this way, we can reproduce the temperature and frequency dependence of the ac susceptibility of SCMs, measured in moderate static fields ($H_{dc} \leq 2$ kOe) and in the presence of crystal defects and/or nonmagnetic impurities. For static fields in this range,

the present data for the relaxation time of the magnetization of CoPhOMe, τ versus H_{dc} , are analyzed at low temperature. They are qualitatively reproduced by theory, provided that finite-size effects are included.

The paper is organized as follows. In Sec. II we present both the real system and the simplified model that we adopt to catch the essentials of its stochastic dynamics. In Sec. III we calculate, for pure and doped chain systems, the temperature dependence of the magnetization and static susceptibility in the presence of a static magnetic field. In Sec. IV, the theoretical framework for the calculation of the dynamic susceptibility in the presence of a static magnetic field is first developed for the infinite chain and then generalized to an open, finite chain with N spins; next we present and discuss the approximation of a single dominating contribution for each segment length, with characteristic frequency Ω_c dependent on N , to the calculation of dynamic susceptibility. In Sec. V, the results of our explicit calculations, performed using parameters suitable for describing CoPhOMe, are shown and discussed. Finally, the conclusions are drawn in Sec. VI, and some technical details are reported in the Appendix, for the reader's convenience.

II. THE MODEL

The magnetic properties of CoPhOMe are determined by Co(II) ions, with an Ising character and effective $S = 1/2$, and by NITPhOMe organic radicals, magnetically isotropic and with $s = 1/2$.^{10,23,31} The primitive magnetic cell is made up of three cobalt ions and three radicals. The spins are arranged in a helical structure, with the helix axis coincident with the crystallographic c axis of the chain; the local axes, along which the spins are aligned, form the same angle $\theta \approx 55^\circ$ with the c axis. The gyromagnetic factor g_R of the organic radical is isotropic, while cobalt is strongly anisotropic, with $g_{Co}^{\parallel} \gg g_{Co}^{\perp}$. The nearest-neighbor exchange between the components of the spins along the local axes is antiferromagnetic,²³ and since the gyromagnetic factors of the two types of magnetic center are different, the sublattice magnetizations are not compensated along c , whereas they are compensated within the plane perpendicular to the chain axis.

Thanks to its ferrimagnetic and quasi-one-dimensional character (the ratio between interchain and intrachain exchange constants is less than 10^{-6}),¹⁰ CoPhOMe was the first magnetic molecular compound to display slow relaxation of the magnetization at low temperatures for $H = 0$,¹⁰ a feature which was predicted a long time ago by Glauber² in a one-dimensional model of Ising spins, coupled by a nearest-neighbor ferromagnetic exchange and interacting with a heat reservoir, causing them to change their states randomly with time.

In this paper we are primarily concerned with analyzing finite-size effects on the spin dynamics of CoPhOMe in the presence of a non-negligible static magnetic field parallel to the chain axis. Since the model of an Ising ferrimagnet with canted spins and two kinds of magnetic center^{23,32} is too involved, in the following we adopt a simplified model, yet able to catch the essentials of the dynamic behavior. Namely, we make the approximation of an open Ising chain with N equal spins, all with $\sigma = \pm 1$ and the same (isotropic) gyromagnetic factor g , coupled by an effective nearest-neighbor ferromagnetic

exchange $J_1 > 0$ and subject to a time-dependent external magnetic field $H(t)$,

$$\mathcal{H} = - \sum_{j=1}^N [J_1 \sigma_j \sigma_{j+1} + g \mu_B H(t) \sigma_j]. \quad (4)$$

Within this model, the spins are supposed to be collinear with the chain axis and with the direction of the applied magnetic field.

It is worth noticing that many single-chain magnets studied so far were rather described by a Heisenberg model with a uniaxial single-ion anisotropy $D > 0$,^{13,14}

$$\mathcal{H} = - \sum_{j=1}^N [J \mathbf{S}_j \cdot \mathbf{S}_{j+1} + D (S_j^z)^2 + g \mu_B \mathbf{H} \cdot \mathbf{S}_j], \quad (5)$$

where $J > 0$ is the ferromagnetic exchange constant between the spins \mathbf{S}_j . For such systems, a description in terms of Glauber dynamics was shown³³ to be valid provided that the ratio between anisotropy and exchange is sufficiently strong: $D/J > 2/3$. In fact, in this case, the energy required to create a Bloch wall depends only on J , and the domain wall is localized on one unit cell (sharp wall).³⁴ For $D/J < 2/3$, the creation energy depends on both J and D , and the domain wall spreads over several lattice spacings.³⁵ The static and dynamic properties of single-chain magnets in such a broad-wall regime were recently investigated³⁶ using transfer matrix calculations and time-quantified Monte Carlo simulations on classical spin chains in the thermodynamic limit ($N \rightarrow \infty$) and for $H = 0$.

In contrast, CoPhOMe represents quite a peculiar example of a single-chain magnet whose static and dynamic properties cannot be described by the model (5). In fact, no experimental evidence for a single-ion uniaxial anisotropy was found in CoPhOMe,^{11,26} neither was it expected, since the Co(II) magnetic centers have effective spin 1/2.

Nevertheless, clear experimental evidence for a strong Ising-like anisotropy in nominally pure CoPhOMe was found for $T < 55$ K, with finite-size effects becoming important for $T < 26$ K.²⁶ Therefore, a strong anisotropy in the exchange coupling has to be invoked for this single-chain magnet. In a classical picture, this means that the z components of the spins experience a much stronger exchange interaction than the x and y components. Then, provided that temperatures are low with respect to exchange coupling, the choice of model (4) is convenient since it allows a simple, though approximated, theoretical description of the spin dynamics of CoPhOMe in the framework of Glauber's theory.² As temperature increases, a description in terms of effective spin 1/2 no longer holds, because higher-energy electronic levels of the metallic centers become populated,²⁶ and the above approximation does not apply.

III. STATIC PROPERTIES

For pure CoPhOMe, static magnetization measurements were originally performed in single-crystal samples¹⁰ with a static magnetic field $H_{dc} = 1$ kOe applied parallel to the chain direction. A strong increase in the quantity TM/H_{dc} is found, upon decreasing T below 100 K, with a maximum reached around 25 K and a subsequent decrease. Such a

behavior, typical of ferromagnetic and ferrimagnetic systems, was also observed in the case of polycrystalline powder samples of pure³⁷ and Zn(II)-doped CoPhOMe,³⁸ at different static magnetic fields and different concentrations of Zn(II) nonmagnetic impurities. It is also a common feature of all SCMs identified so far.¹⁴

For a finite chain of N spins, coupled by the Hamiltonian (4) and subject to open boundary conditions, the static properties in a time-independent field H_{dc} can be calculated analytically by the transfer matrix method.³ The free energy F_N can be expressed as the sum of a bulk, a surface, and a finite-size contribution:³⁹

$$F_N = -k_B T \{ N \ln \lambda_{>} + \ln(a_{>}/\lambda_{>}) + \ln[1 + (a_{<}/a_{>})(\lambda_{<}/\lambda_{>})^{N-1}] \}. \quad (6)$$

The two eigenvalues $\lambda_{\geq} = e^K (\cosh h_0 \pm \Delta^{1/2})$ and the two coefficients $a_{\geq} = \cosh h_0 \pm \Delta^{-1/2} (\sinh^2 h_0 + e^{-4K})$ related to the two eigenvectors are expressed in terms of the Hamiltonian parameters in Eq. (4) by $K = \frac{J_1}{k_B T}$, $h_0 = \frac{g \mu_B H_{dc}}{k_B T}$, and $\Delta = \sinh^2 h_0 + e^{-4K}$.

For a doped chain with a given concentration c of nonmagnetic impurities, the magnetization per spin, M_{doped} , and static susceptibility per spin, χ_{doped} , are, respectively

$$M_{\text{doped}} = \sum_{N=1}^{\infty} c^2 (1-c)^N M_N, \quad (7)$$

$$\chi_{\text{doped}} = \sum_{N=1}^{\infty} c^2 (1-c)^N \chi_N,$$

where the static magnetization M_N and static susceptibility χ_N of a finite open Ising chain with N spins are obtained from Eq. (6) simply by deriving F_N with respect to the static magnetic field

$$M_N = - \frac{\partial F_N}{\partial H_{dc}}, \quad \chi_N = - \frac{\partial^2 F_N}{\partial H_{dc}^2}. \quad (8)$$

For the infinite chain (i.e., $c = 0$ and $N \rightarrow \infty$), according to Eq. (6) the static properties can be calculated analytically^{3,39} in terms only of the larger eigenvalue $\lambda_{>}$. In particular, the magnetization per spin is

$$m = k_B T \frac{1}{\lambda_{>}} \frac{\partial \lambda_{>}}{\partial H_{dc}} = \Delta^{-1/2} \sinh h_0 \equiv m_{\text{eq}}, \quad (9)$$

and the susceptibility per spin is $\chi_{\infty} = \frac{\partial m}{\partial H_{dc}}$. In a nonzero static field, χ_{∞} is found to be exponentially vanishing for $T \rightarrow 0$ [see Eq. (22) later on], in strong contrast with the exponentially diverging low- T behavior of the same quantity in $H_{dc} = 0$.

In Fig. 1 the calculated quantity TM/H_{dc} is reported versus T for different values of c (including $c = 0$) and for a fixed value of the dc field ($H_{dc} = 1$ kOe). In Fig. 2, the same quantity is reported for different values of the static applied magnetic field and for a fixed, rather small, value of the nonmagnetic impurity concentration ($c = 0.01$). It is worth observing that, at low fields and low temperatures, the curves calculated for $c = 0.01$ resemble the experimental ones, obtained by Lascialfari *et al.*³⁷ for a powder sample of nominally pure CoPhOMe (see inset). In contrast, according to Eq. (9), the theoretical curves

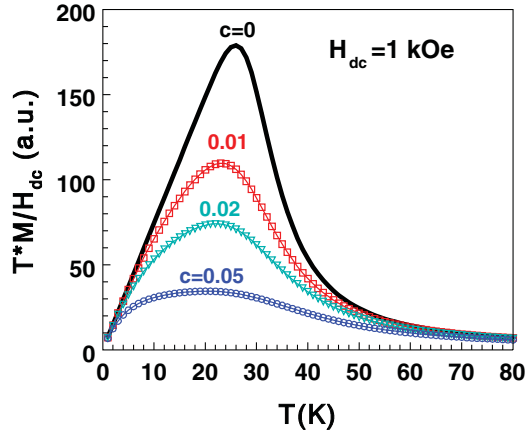


FIG. 1. (Color online) TM/H_{dc} versus T for an Ising chain with $J_I/k_B = 80$ K, in a static magnetic field $H_{dc} = 1$ kOe, calculated for selected values of the concentration c of nonmagnetic impurities (different symbols refer to $c = 0.05, 0.02, 0.01$ on going from bottom to top), and for the pure system ($c = 0$, full line).

for the pure system (not shown here) are found to undergo a much stronger increase at such low fields and temperatures (as can also be inferred from the concentration dependence of TM/H_{dc} shown in Fig. 1). Previous suggestions^{24–26} about the presence of lattice imperfections, or impurities that limit the chain size even in pure CoPhOMe, appear thus to be confirmed.

In Fig. 3 we show experimental data for the temperature dependence of $\chi'(\omega)$, the real part of the ac susceptibility of a nominally pure CoPhOMe sample, measured at frequency $\nu = 1$ kHz for a fixed value of the static applied field, $H_{dc} = 1$ kOe. For the same field, the calculated static susceptibility χ_∞ of the infinite chain ($c = 0$, full line) is exponentially vanishing at low temperatures, in strong contrast with the diverging behavior of χ_∞ in zero field. For the doped chain ($c = 0.047$, dashed line), the static susceptibility χ_{doped} was calculated in the framework of the simplified model (4). As observed in previous work,³² a precise relationship is still lacking between

the Hamiltonian parameters of the original ferrimagnetic model of CoPhOMe and those of model (4). Using an effective exchange $J_I = 80$ K and an effective gyromagnetic factor $g = 2$, we found that χ_{doped} , as given in Eq. (7), turns out to be in nice agreement with previous results from an exact transfer matrix calculation, performed for the more complete model of a ferrimagnetic chain with two kinds of spin with different gyromagnetic factors.²⁶ In particular, the model (4) allows us to recover the feature of a peak, in χ_{doped} versus T , gradually shifting to lower temperatures with increasing c : a clear signature of finite-size effects (not shown here). From Fig. 3 one sees that the two-peaked feature, experimentally observed at nonzero field in $\chi'(\omega)$ versus T , can be well reproduced by taking a weighted average (light-gray triangles) between the static susceptibility of the pure chain (χ_∞ , full line) and that of the doped one (χ_{doped} , dashed line). Finally we mention that the steep decrease, displayed by the experimental $\chi'(\omega)$ for $T \leq 10$ K, can also be well reproduced (blue circles) by taking into account dynamic effects, at it will be shown in Sec. IV. In summary, the data and calculations reported in Fig. 3 not only are in good agreement with the reported presence of a distribution of impurities inside the crystal,²⁶ but are also revealing of a nonhomogeneous nature of the samples.

A similar two-peaked feature was observed, later, in the real part of the ac susceptibility of a different cobalt-organic single-chain magnet, for $H_{dc} = 0.5$ kOe.²⁷ As in the case of CoPhOMe, the higher-temperature peak, due to the infinite chain, did not present any dynamic effect, while the lower-temperature shoulder, related to finite-size effects, was found to be frequency dependent. In the following we will show that the latter feature can be well accounted for by a calculation of the dynamic susceptibility in the framework of the simplified model (4).

IV. DYNAMIC PROPERTIES

In ac magnetic measurements, a small ac drive magnetic field is superimposed on the dc field, causing a time-dependent moment in the sample. Therefore we are faced with the theoretical problem of determining how the kinetic equations of motion for the time-dependent spin averages of a finite, open chain in zero magnetic field^{21,22} are modified by the presence of a magnetic field of the general form

$$H(t) = H_{dc} + H_1 e^{-i\omega t}, \quad (10)$$

i.e., the sum of a static dc field of any intensity, H_{dc} , and of an ac field, oscillating at the angular frequency ω . In the following we will make use of the reduced fields $h_0 = \frac{g\mu_B H_{dc}}{k_B T}$ and $h_1 = \frac{g\mu_B H_1}{k_B T}$. As the experimental oscillating fields are usually much smaller than the static field, we will consider the case $H_1 \ll H_{dc}$, which allows us to use the expansion $[h(t) = \frac{g\mu_B H(t)}{k_B T}]$

$$\tanh h(t) \approx \tanh h_0 + h_1 e^{-i\omega t} (1 - \tanh^2 h_0). \quad (11)$$

Generally speaking, the susceptibility induced by a field as in Eq. (10) will have a real and an imaginary part,

$$\chi(\omega) = \chi'(\omega) + i\chi''(\omega), \quad (12)$$

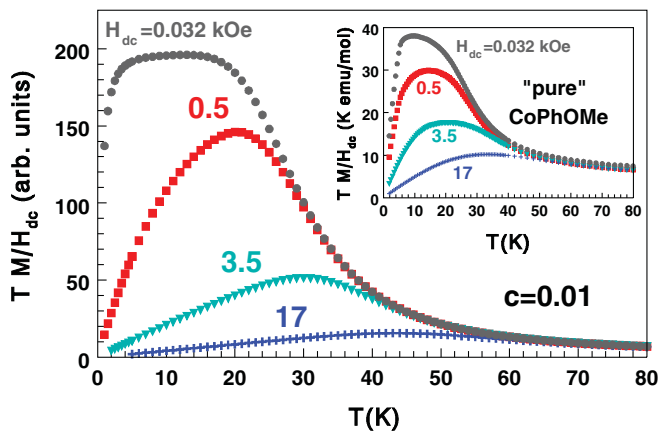


FIG. 2. (Color online) TM/H_{dc} versus T for a doped Ising chain with $J_I/k_B = 80$ K, calculated for different values of the static applied field, at a fixed value ($c = 0.01$) of the nonmagnetic impurities concentration. Inset: Experimental data for a nominally pure ($c = 0$) powder sample.

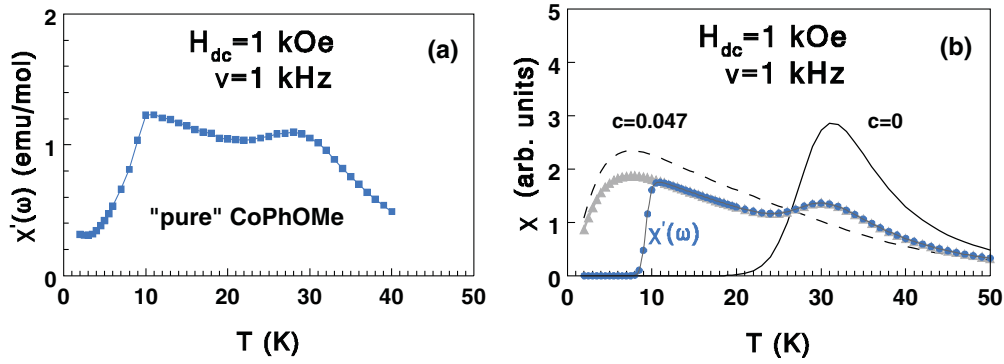


FIG. 3. (Color online) (a) Real part of the ac susceptibility, $\chi'(\omega)$ (square symbols), measured versus temperature in a nominally pure CoPhOMe sample for frequency $\nu = 1$ kHz and fixed static applied field $H_{dc} = 1$ kOe. (b) Static susceptibility χ calculated with $J_I/k_B = 80$ K and $H_{dc} = 1$ kOe, for a doped Ising chain (χ_{doped} , dashed line, $c = 0.047$) and for an infinite chain (χ_{∞} , full line, $c = 0$). The two-peaked structure (light-gray triangles) is obtained by taking a weighted average of the two quantities (80% versus 20%, respectively). The real part of the dynamic susceptibility, $\chi'(\omega)$, calculated according to the theory in Sec. IV, is denoted by blue circles.

from which the dynamic behavior of molecular materials is usually extracted. In the following we will thus focus on calculating these experimentally relevant quantities, which are compared to data in the next section.

Typical values of the frequencies $\nu = \frac{\omega}{2\pi}$ used in ac susceptibility measurements^{10,26} on pure and doped CoPhOMe range between 0.1 and 10 000 Hz. In contrast, one has $\nu \approx$ MHz for proton nuclear magnetic resonance (NMR) and muon spin relaxation (μ SR) experiments.^{40,41} In the following, before passing to the comparison with experimental data, we first examine the properties of an infinite chain (Sec. IV A), then include finite-size effects (Sec. IV B), and eventually explore the single-frequency approximation (Sec. IV C).

A. Infinite chain

Before considering finite-size effects, it is instructive to calculate first the dynamic susceptibility of an infinite Ising chain in the presence of a static magnetic field. The kinetic equation for the site-independent average $m(t) = \langle \sigma(t) \rangle$ of a spin in the infinite chain is

$$\tau_0 \frac{dm(t)}{dt} = -(1 - \gamma)m(t) + [1 - \gamma\Gamma_1(t)] \tanh h(t), \quad (13)$$

where $\gamma = \tanh(2K)$ and $\Gamma_1(t)$ is the nearest-neighbor spin-pair time-dependent correlation function. The kinetic equation for $\Gamma_1(t)$, in its turn, involves higher-order time-dependent correlation functions, so that eventually an infinite sequence of equations is obtained as a consequence of $h(t) \neq 0$. In order to truncate this hierarchy, we adopt the local-equilibrium approximation:^{29,30} i.e., the relation holding at equilibrium⁴² between the nearest-neighbor correlation function and the magnetization [where m_{eq} is defined in Eq. (9)],

$$\Gamma_{1,\text{eq}} = 1 - \frac{2(1 - m_{\text{eq}}^2)}{1 + \sqrt{m_{\text{eq}}^2 + (1 - m_{\text{eq}}^2)e^{4K}}}, \quad (14)$$

is assumed to hold *locally* also at any time $t \neq 0$. The main advantages of this approximation, first proposed by Huang³⁰ for an infinite Ising chain model with Glauber dynamics in $H_{dc} \neq 0$, are that (i) it provides the exact steady-state

solution,³⁰ in contrast with the mean-field approximation, which assumes simply $\Gamma_{1,\text{eq}} = m_{\text{eq}}^2$; (ii) it is valid for any value of the applied field, in contrast with the perturbation method, which assumes $h_0 \ll 1$.²

In this way, a nonlinear equation for $m(t)$ is obtained, where the approximation of a linear response of the chain applies only to the ac field H_1 . We thus assume $\delta m(t) = m(t) - m_{\text{eq}}$, i.e., small departures of the magnetization from its equilibrium value m_{eq} . Likewise, we expand $\Gamma_1(t) \approx \Gamma_1|_{\text{eq}} + \frac{d\Gamma_1(t)}{dm(t)}|_{\text{eq}} \delta m(t)$ and, taking into account that $\frac{d\Gamma_1(t)}{dm(t)}|_{\text{eq}} = 2 \tanh h_0$ at equilibrium,²⁹ we finally obtain a linear nonhomogeneous differential equation for $\delta m(t)$,

$$\tau_0 \frac{d\delta m(t)}{dt} = -(1 - \gamma + 2\gamma \tanh^2 h_0)\delta m(t) + h_1 e^{-i\omega t} (1 - \tanh^2 h_0)(1 - \gamma\Gamma_{1,\text{eq}}). \quad (15)$$

In the absence of the ac field ($h_1 = 0$), one finds an exponential time decrease for the magnetization fluctuation,

$$\delta m(t) = \delta m(t_0) e^{-\lambda_{\infty}(t-t_0)/\tau_0}. \quad (16)$$

Thus, for the infinite Ising chain, there is a single relaxation time τ_{∞} related to the adimensional parameter λ_{∞} by

$$\lambda_{\infty} = \frac{\tau_0}{\tau_{\infty}} = 1 - \gamma + 2\gamma \tanh^2 h_0. \quad (17)$$

Notice that, for $h_0 \rightarrow 0$, Glauber's result² of an exponentially diverging relaxation time at low temperatures ($\tau_{\infty} \approx \frac{1}{2}\tau_0 e^{4K}$ for $k_B T \ll J_I$) is correctly recovered, while for $H_{dc} \neq 0$ the relaxation time of the infinite chain does not diverge any more.

In the presence of the ac field ($h_1 \neq 0$), the general solution of Eq. (15) is

$$\delta m(t) = \delta m(t_0) e^{-\lambda_{\infty}(t-t_0)/\tau_0} + h_1 (1 - \tanh^2 h_0) \times (1 - \gamma\Gamma_{1,\text{eq}}) \int_{t_0}^t e^{-i\omega t'} e^{-\lambda_{\infty}(t-t')/\tau_0} dt'. \quad (18)$$

Taking into account that $\lambda_\infty \neq 0$, one can safely let $t_0 \rightarrow -\infty$ in order to find a solution that does not depend on the initial conditions,^{2,43}

$$\delta m(t) = (1 - \tanh^2 h_0)(1 - \gamma \Gamma_{1,\text{eq}}) \frac{h_1 e^{-i\omega t}}{\lambda_\infty - i\omega \tau_0}. \quad (19)$$

The fluctuation of the total magnetization of the infinite Ising chain is obtained by summing over all the N spins and letting $N \rightarrow \infty$,

$$\delta \langle M(t) \rangle = N g \mu_B \delta \langle \sigma(t) \rangle = \chi(\omega) H_1 e^{-i\omega t}, \quad (20)$$

so that the dynamic susceptibility $\chi(\omega)$ is

$$\begin{aligned} \chi(\omega) &= \frac{g^2 \mu_B^2 N}{k_B T} (1 - \tanh^2 h_0) (1 - \gamma \Gamma_{1,\text{eq}}) \\ &\times \frac{1}{\lambda_\infty - i\omega \tau_0} = \frac{\chi_\infty}{1 - i\omega \frac{\tau_0}{\lambda_\infty}}, \end{aligned} \quad (21)$$

where χ_∞ denotes the static susceptibility of the infinite Ising chain for $H_{\text{dc}} \neq 0$,

$$\chi_\infty = \frac{g^2 \mu_B^2 N}{k_B T} \frac{(1 - \tanh^2 h_0)(1 - \gamma \Gamma_{1,\text{eq}})}{1 - \gamma + 2\gamma \tanh^2 h_0}. \quad (22)$$

For $h_0 \rightarrow 0$, Glauber's result²

$$\chi(\omega) = \frac{g^2 \mu_B^2 N}{k_B T} \frac{1 + \eta}{1 - \eta} \frac{1}{1 - i\omega \frac{\tau_0}{1 - \gamma}} \quad (23)$$

is correctly recovered, by taking into account that $\lambda_\infty \rightarrow 1 - \gamma$, $\Gamma_{1,\text{eq}} \rightarrow \eta = \tanh K$, and $\gamma = \frac{2\eta}{1 + \eta^2}$.

B. Finite chain

In the case of an open Ising chain with a finite number N of spins, the lack of translational invariance leads to N kinetic equations for the N site-dependent spin averages $\delta \langle \sigma_p(t) \rangle$ ($p = 1, \dots, N$).^{21,22,29} As in the case of the infinite chain, we can introduce the local-equilibrium approximation^{29,30} in order to truncate the infinite sequence of equations for the higher-order time-dependent spin correlation function. Next we perform the linearization of the kinetic equations, in the hypothesis of a linear response to the ac magnetic field. We then obtain a set of N linear differential equations, which can be written in matrix form as

$$\tau_0 \frac{d\mathbf{\Sigma}}{dt} = -\mathbf{Y} \cdot \mathbf{\Sigma} + h_1 e^{-i\omega t} (1 - \tanh^2 h_0) \mathbf{\Psi}, \quad (24)$$

where $\mathbf{\Sigma}$ and $\mathbf{\Psi}$ are $N \times 1$ vectors containing the spin fluctuations and the nonhomogeneous terms, respectively (see the Appendix for details). \mathbf{Y} is a real, symmetric, tridiagonal $N \times N$ matrix, with nonzero adimensional eigenvalues λ_j ($j = 1, \dots, N$), while $\Phi^{(\lambda_j)}$ are the corresponding $N \times 1$ eigenvectors. In the limiting case $h_0 \rightarrow 0$, the numerical solutions for λ_j coincide with the ones obtained^{21,22} in the framework of a finite-size scaling calculation of the Glauber dynamics in a zero static field. In particular, the low-temperature expansion ($k_B T \ll J_1$) for the eigenvalue of a finite open chain with N spins is $\lambda_1(H_{\text{dc}} = 0) \approx \frac{2}{N-1} e^{-2J_1/k_B T}$,²¹ to be compared with $\lambda_\infty(H_{\text{dc}} = 0) \approx 2e^{-4J_1/k_B T}$ for the eigenvalue of the infinite chain.²

We are interested in the long-time behavior of the system, characterized for being independent of the initial condition. Thus, solving Eq. (24) by the method of eigenfunctions^{44,45} and letting $t_0 \rightarrow -\infty$,^{2,43} we obtain for the fluctuation of a single-spin average ($p = 1, \dots, N$)

$$\begin{aligned} \delta \langle \sigma_p(t) \rangle &= h_1 e^{-i\omega t} (1 - \tanh^2 h_0) \\ &\times \sum_{j=1}^N \frac{1}{\lambda_j - i\omega \tau_0} \Phi_p^{(\lambda_j)} \left(\sum_{m=1}^N \Phi_m^{(\lambda_j)} \Psi_m \right). \end{aligned} \quad (25)$$

The fluctuation of the magnetization of the finite open Ising chain is obtained by summing over the N spins

$$\delta \langle M_N(t) \rangle = g \mu_B \sum_{p=1}^N \delta \langle \sigma_p(t) \rangle = \chi_N(\omega) H_1 e^{-i\omega t}. \quad (26)$$

The dynamic susceptibility $\chi_N(\omega)$ takes the form

$$\chi_N(\omega) = \frac{g^2 \mu_B^2}{k_B T} \sum_{j=1}^N \frac{\Omega_j^2 + i\omega \Omega_j}{\Omega_j^2 + \omega^2} A_j(\lambda_j, T, H_{\text{dc}}) \quad (27)$$

where the angular frequencies are ($j = 1, \dots, N$)

$$\Omega_j = \frac{\lambda_j}{\tau_0} \quad (28)$$

and the corresponding frequency weights are

$$A_j(\lambda_j, T, H_{\text{dc}}) = \frac{1 - \tanh^2 h_0}{\lambda_j} \sum_{p=1}^N \Phi_p^{(\lambda_j)} \left(\sum_{m=1}^N \Phi_m^{(\lambda_j)} \Psi_m \right). \quad (29)$$

The angular frequencies (28) are expressed in terms of the adimensional eigenvalues λ_j of the matrix \mathbf{Y} and of the characteristic time τ_0 for the spin flip of an isolated spin. The latter is a free parameter which is expected to depend, in general, on the intensity of the applied magnetic field.²⁹ The general expression for the dynamic susceptibility per spin of a doped chain is thus

$$\chi(\omega) = \sum_{N=1}^{\infty} c^2 (1 - c)^N \chi_N(\omega). \quad (30)$$

C. Single-frequency approximation

Let us start by deriving a quite general sum rule for the frequency weights, which is readily obtained by setting zero frequency ($\omega = 0$) in Eq. (27),

$$\sum_{j=1}^N A_j(\lambda_j, T, H_{\text{dc}}) = \frac{k_B T}{g^2 \mu_B^2} \chi_N, \quad (31)$$

where χ_N , the static susceptibility of a finite, open Ising chain with N spins, subject to the dc field H_{dc} , is given in Eq. (8). Next we observe that, in the approximation of a single characteristic frequency Ω_c dominating the relaxation of the magnetization fluctuations of a segment with fixed length, Eq. (27) for the dynamic susceptibility of a finite, open, Ising chain with N spins assumes the simple form

$$\chi_N(\omega) \approx \chi_N \frac{\Omega_c^2 + i\omega \Omega_c}{\Omega_c^2 + \omega^2}. \quad (32)$$

In principle, the characteristic frequency is not necessarily $\Omega_c = \lambda_1/\tau_0$, i.e., related to the smallest eigenvalue of \mathbf{Y} . Rather, in order to determine the dominating frequency, the temperature dependence of the frequency weights must be taken into account.⁴⁶

For a doped chain, when the single-frequency approximation is performed for each chain segment with N spins, the dynamic susceptibility per spin assumes the simplified form

$$\chi(\omega) \approx \sum_{N=1}^{\infty} c^2(1-c)^N \chi_N \frac{\Omega_c^2 + i\omega\Omega_c}{\Omega_c^2 + \omega^2}, \quad (33)$$

where χ_N is given in Eq. (8), and we recall that the characteristic frequency Ω_c depends on N .

Finally we observe that, using the fluctuation-dissipation theorem, the linear response $S_N(\omega)$ of a finite, open Ising chain with N spins can be expressed as a weighted sum of N Lorentzian functions, centered at zero frequency, with widths Ω_j ,

$$S_N(\omega) = \frac{2k_B T}{\omega} \chi_N''(\omega) = 2g^2 \mu_B^2 \sum_{j=1}^N \frac{\Omega_j}{\Omega_j^2 + \omega^2} A_j(\lambda_j, T, H_{dc}). \quad (34)$$

When the approximation of a single dominating frequency (32) holds, the linear response is simply the product of $T \chi_N$ and of a single Lorentzian function, centered at zero frequency, with width equal to the characteristic frequency Ω_c ,

$$S_N(\omega) = \frac{2k_B T}{\omega} \chi_N''(\omega) \approx 2k_B T \chi_N \frac{\Omega_c}{\Omega_c^2 + \omega^2}. \quad (35)$$

It is worth noticing that expressions quite similar to Eqs. (34) and (35) were obtained for the spectrum of fluctuations of a cluster magnetization by Santini *et al.*,⁴⁶ in the framework of an exact calculation of the energy levels of three important classes of magnetic molecules in contact with a phonon heat bath: namely, antiferromagnetic rings, grids, and nanomagnets. Moreover, Bianchi *et al.*⁴⁷ recently showed that, while for antiferromagnetic homometallic rings the approximation of a single dominating frequency is valid, it does not hold for heterometallic rings,⁴⁶ due to the presence of inequivalent ions which prevent mapping local-spin correlations with the corresponding total-spin ones.

V. RESULTS

In this section we compare the theoretical results derived in Sec. IV with experimental ac susceptibility data, obtained in nominally pure and zinc-doped CoPhOMe for different values of H_{dc} and of the frequency of the oscillating field. Also, our experimental data for the relaxation time of the magnetization, measured as a function of the static magnetic field at fixed temperature, will be discussed and compared with theoretical calculations.

Let us first provide evidence for the correctness of the single-frequency approximation, Eq. (32), by showing the temperature dependence of the eigenvalues and weights of a finite, open, Ising chain in an applied dc field. The values of the Hamiltonian parameters we assumed for the dynamic calculations, $J_I/k_B = 80$ K and $g = 2$, are the same we used

in Sec. III for the static properties. The characteristic time for the spin flip of an isolated spin, τ_0 , was left as a free parameter (see later on). Moreover, the field dependence of τ_0 , though expected in principle,²⁹ was neglected for the sake of simplicity.

In Fig. 4 some of the calculated adimensional eigenvalues λ_j ($j = 1, \dots, N$) of the real tridiagonal matrix \mathbf{Y} , defined in Eqs. (24) and (A10), are reported as a function of inverse temperature for different values of the number of spins N and of the applied static field H_{dc} . For the sake of comparison, the temperature dependence of the eigenvalue λ_∞ [see Eq. (17)] of an infinite chain in the same field is also shown. Except for the case of long chains and strong fields, at sufficiently low temperatures a single mode dominates the low-frequency dynamics of a finite, open, Ising chain with N spins: namely, the mode with characteristic frequency $\Omega_c = \lambda_1/\tau_0$, where λ_1 is the smallest eigenvalue of \mathbf{Y} . The temperature dependence of the frequency weights corresponding to the various modes is displayed in the insets of Fig. 4: for not too long chains and not too strong fields, one can see that the frequency related to the smallest eigenvalue λ_1 has the strongest weight.

A. ac Susceptibility

Some years ago, the ac susceptibility of CoPhOMe was measured versus T in single crystals, both for $H_{dc} = 0$ Oe in a nominally pure sample¹⁰ and for $H_{dc} = 2$ kOe in a doped one.²⁶ In this work, we present some data for $\chi(\omega)$ versus T . Data were obtained using a homemade ac probe and a Cryogenics magnetometer, on a collection of nominally pure single crystals of CoPhOMe. The crystals were all aligned with the chain axis along the magnetic field direction. The frequencies in an ac susceptibility experiment typically range between 0.1 and 10 kHz, and we can safely adopt the single-frequency approximation in order to account for the temperature dependence of $\chi(\omega)$ in moderate fields ($H_{dc} \leq 2$ kOe). Additionally the oscillating fields used were always below 8 Oe, and the condition $H_{dc} \gg H_1$ is also fulfilled.

In Figs. 5(a) and 5(b) we show the temperature dependence of the real and imaginary parts of the dynamic susceptibility calculated for an infinite chain with $H_{dc} = 0$, while analogous quantities calculated for a zinc-doped chain ($c = 0.047$) in $H_{dc} = 2$ kOe are reported in Figs. 5(c) and 5(d).

In the pure system ($c = 0$) with $H_{dc} = 0$, the static susceptibility [full black curve in Fig. 5(a)] diverges as $T \rightarrow 0$. As regards the dynamic susceptibility (23) [colored curves in Figs. 5(a) and 5(b)], a single, resonating peak is found for both $\chi'(\omega)$ and $\chi''(\omega)$ versus T ; the peak position gradually shifts to higher temperature with increasing frequency of the tiny oscillating field. The phenomenon can be interpreted^{32,43,48} as a manifestation of stochastic resonance in a set of coupled bistable systems: i.e., there is an optimal value of noise, for which the response of the dynamic system to the driving field is maximum. In a ferromagnetic or ferrimagnetic chain, the role of stochastic noise is played by thermal fluctuations, and a resonance peak occurs when the deterministic time scale of the oscillating magnetic field matches the statistical time scale associated with the spontaneous decay of the net magnetization.

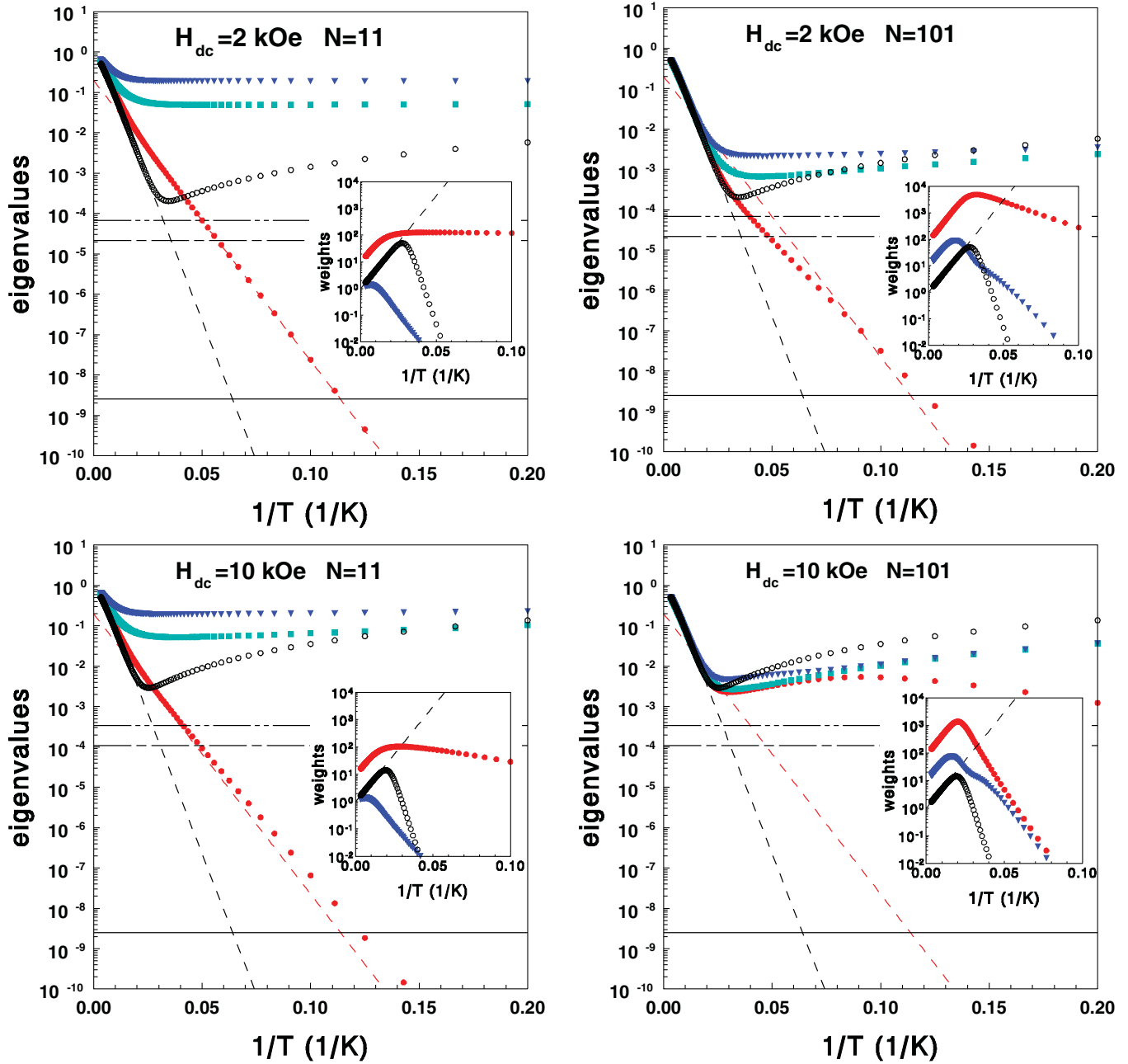


FIG. 4. (Color online) Temperature dependence of the first three eigenvalues $\lambda_j = \Omega_j \tau_0$ ($j = 1$, red full circles; $j = 2$, green full squares; $j = 3$, blue full triangles) of an open Ising chain, calculated for a finite number of spins ($N = 11$ and $N = 101$) in presence of a nonzero static field ($H_{dc} = 2$ kOe and $H_{dc} = 10$ kOe). For comparison, the eigenvalue λ_∞ (black open circles) of an infinite chain in nonzero field is also reported. Dashed lines denote the zero-field, low-temperature expansions for the smallest eigenvalue of a finite chain, $\lambda_1(H_{dc} = 0) \approx \frac{2}{N-1} e^{-2J_1/k_B T}$ (Ref. 21) and for the eigenvalue of an infinite chain, $\lambda_\infty(H_{dc} = 0) \approx 2e^{-4J_1/k_B T}$ (Ref. 2). The horizontal lines, from bottom to top, denote the quantity $2\pi\nu\tau_0$, calculated for three different frequencies: $\nu = 1$ kHz, ν (MHz) = $4.26 \times H_{dc}$ (kOe), and ν (MHz) = $13.55 \times H_{dc}$ (kOe), typically used in ac susceptibility, proton NMR, and μ SR measurements, respectively. Insets: calculated temperature dependence of the frequency weights $A_j(\lambda_j, T, H_{dc})$ with $j = 1$ and 3 (red full circles and blue full triangles, respectively); for odd N , the weights of the even modes are zero (Ref. 29). The curves denoted by black open circles and black dashed lines represent the frequency weights of an infinite chain in $H_{dc} \neq 0$ and in $H_{dc} = 0$, respectively. The parameters used for the calculations were $J_1/k_B = 80$ K, $g = 2$, and $\tau_0 = 4 \times 10^{-13}$ s.

For the doped system in $H_{dc} = 2$ kOe, we find that a frequency-dependent peak in the calculated $\chi'(\omega)$ and $\chi''(\omega)$ versus T [the colored curves in Figs. 5(c) and 5(d)] develops at substantially lower temperatures with respect to the peak in the static susceptibility of an infinite chain [the full black curve

in Fig. 5(c); see Eq. (22)]. This can be easily understood by looking at Fig. 4: for a finite, open Ising chain in a moderate field, the fulfillment of the resonance condition [$\omega = \Omega_c$ in Eq. (32)] occurs at low temperatures, as signaled by the crossing between the full horizontal line (which represents a

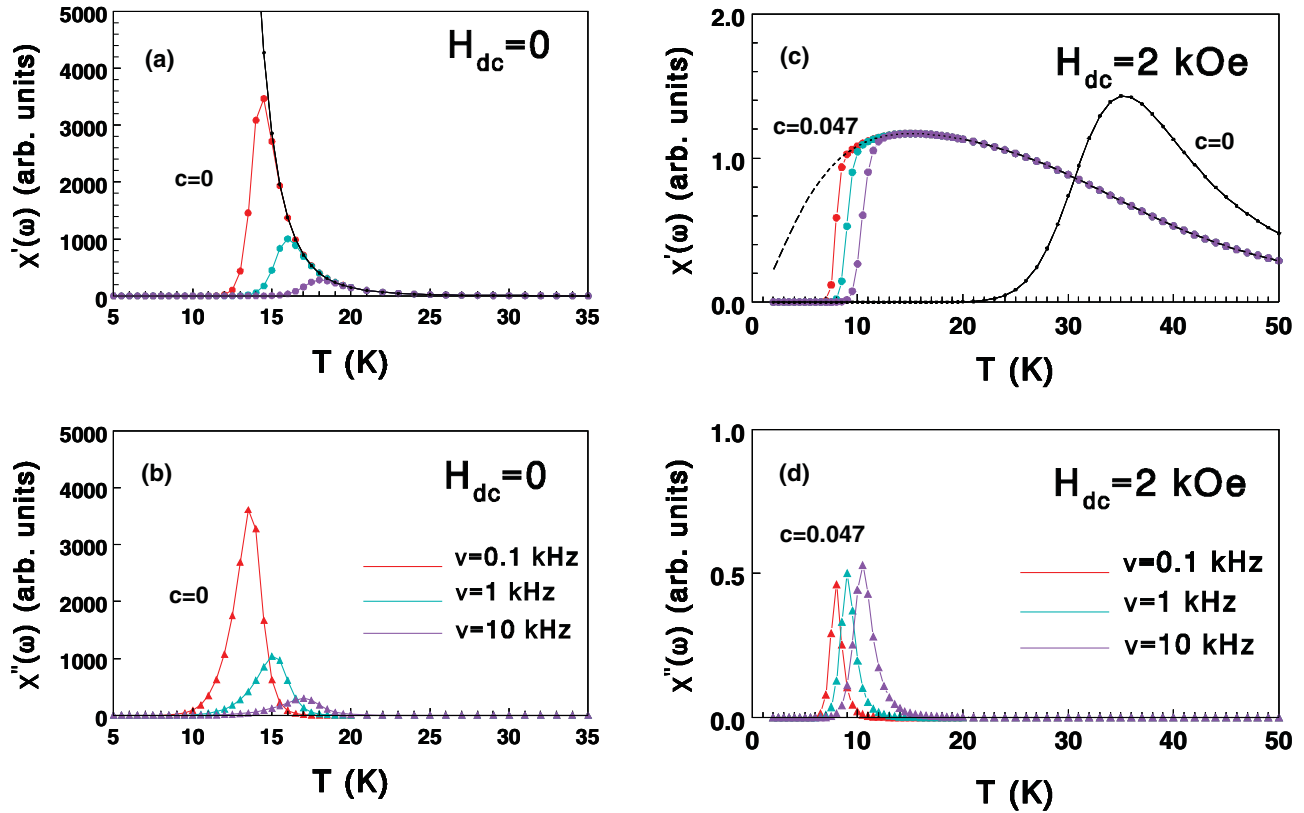


FIG. 5. (Color online) Temperature dependence of the calculated dynamic susceptibility for an infinite ($c = 0$) ferromagnetic Ising chain in zero static field $H_{dc} = 0$ (a) and (b), and of a doped ($c = 0.047$) Ising chain in nonzero static field $H_{dc} = 2$ kOe (c) and (d). The different curves refer to different frequencies ($\nu = 0.1, 1,$ and 10 kHz on going from left to right) of the ac magnetic field. The calculated static susceptibility of the infinite chain in $H_{dc} = 0$ is denoted by the full black line: it diverges exponentially as T is decreased to 0 [see (a)], while in $H_{dc} \neq 0$ it goes through a peak, and then vanishes exponentially [see (c)]. The calculated static susceptibility of the doped ($c = 0.047$) chain in nonzero ($H_{dc} = 2$ kOe) field is denoted by the black dashed line [see (c)].

typical value, 1 kHz, of the frequency ν in an ac susceptibility measurement) and the curve (red full circles) representing the T dependence of the smallest-frequency mode λ_1 . In contrast, the crossing does not occur in the case of an infinite chain (black open circles) subject to the same dc field: i.e., the relaxation rate of the infinite chain does not fulfill the resonance condition [$\omega\tau_0 = \lambda_\infty$ in Eq. (21)] at the low frequencies involved in the ac susceptibility experiment: thus, the infinite chain does not present any dynamic response. As already observed in Sec. III, the nominally pure samples are nonhomogeneous and consequently, at low temperatures, only the regions with dilute chains contribute to the dynamic properties in a significant way. This explains the experimental results^{10,11,23–25} in which the measured relaxation rate, for $H_{dc} = 0$, was always found to follow a modified Arrhenius law with a halved energy barrier, $\tau(T) = \tau_0(\bar{L})e^{2J_1/k_B T}$, where \bar{L} is the mean chain length.

In Fig. 6 we present experimental data for the temperature dependence of the ac susceptibility of CoPhOMe, measured for a fixed value of the frequency ($\nu = 1$ kHz) at different values of the static magnetic field ($H_{dc} \leq 1$ kOe) [Figs. 6(a) and 6(b)], and for a fixed value of the dc field ($H_{dc} = 1$ kOe) at different values of the frequency ($\nu \leq 1$ kHz) [Figs. 6(c) and 6(d)]. In Fig. 7 we plot the real and imaginary parts of the dynamic susceptibility, calculated using Eq. (33) for a doped

chain ($c = 0.047$) at just the same values of frequency and dc field as in Fig. 6. For the sake of comparison, the dynamic susceptibility of the infinite chain ($c = 0$) was also calculated: for fixed $H_{dc} = 1$ kOe, at the chosen values of ν , this quantity was not found to display any frequency dependence [see the black line in Fig. 7(c)], in fine agreement with experimental observations [see the higher-temperature peak in Fig. 6(c)]. Thus we can conclude that, for the moderate values of ν and H_{dc} exploited in the present ac susceptibility experiments, (i) the frequency dependence of $\chi(\omega)$ can be attributed solely to finite-size effects; (ii) the approximation of a single dominating frequency for each segment length is a good one for the calculation of the dynamic susceptibility.

B. Relaxation time

In Fig. 8(a) we show the frequency dependence of the imaginary part of the ac susceptibility, measured for a sample of five crystals of nominally pure CoPhOMe, at a fixed temperature of 9 K and for H_{dc} ranging from 0.1 to 2 kOe. Fitting of the curves was performed using an extended Debye model to extract the peak frequency⁴⁹

$$\chi(\omega) = \chi_s + \frac{\chi_T - \chi_s}{1 + (i\omega\tau)^{1-a}}, \quad (36)$$

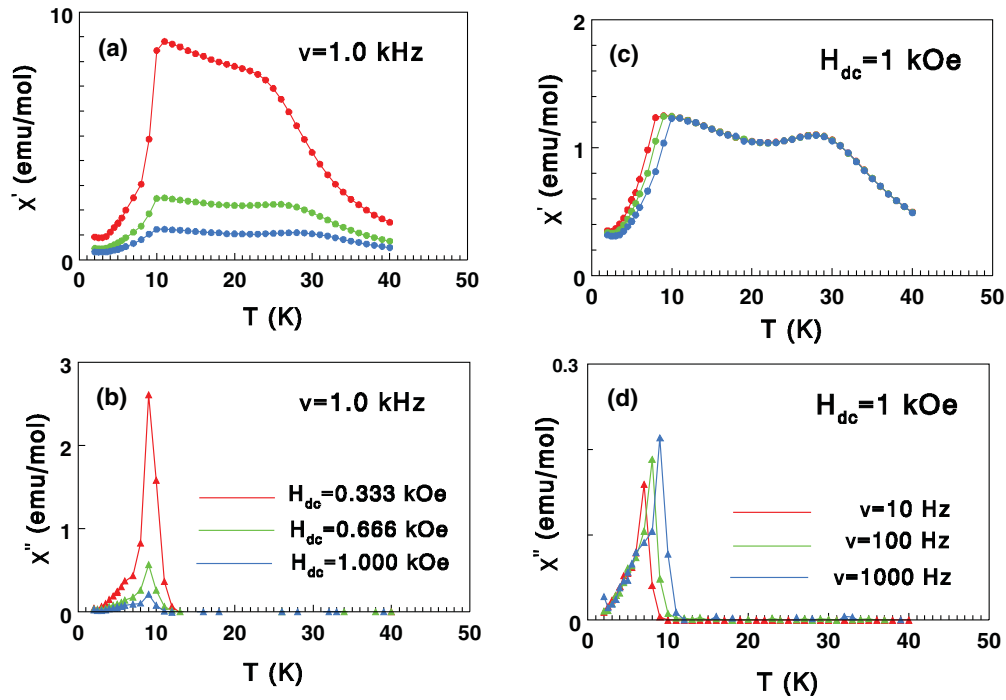


FIG. 6. (Color online) Temperature dependence of the measured ac susceptibility of CoPhOMe. The data refer to the same sample as in Fig. 3(a). In (a) and (b), the frequency was fixed ($\nu = 1$ kHz) and the dc field was varied ($H_{dc} = 0.333, 0.666$, and 1 kOe on going from top to bottom). In (c) and (d), the dc field was fixed ($H_{dc} = 1$ kOe) and the frequency was varied ($\nu = 10, 100$, and 1000 Hz on going from left to right).

where χ_T is the isothermal susceptibility, χ_S is the adiabatic susceptibility, and α is a parameter that measures the distribution of relaxation times in the sample. In the present measurements it was found that $\alpha \approx 0$, meaning that the whole system relaxes with a single characteristic time. The field

dependence of the relaxation time τ , obtained in this way, is reported (red squares) in Fig. 8(b).

The field dependence of the relaxation time at a lower temperature, $T = 5.1$ K, was instead obtained by performing dc measurements. The magnetization was first saturated in

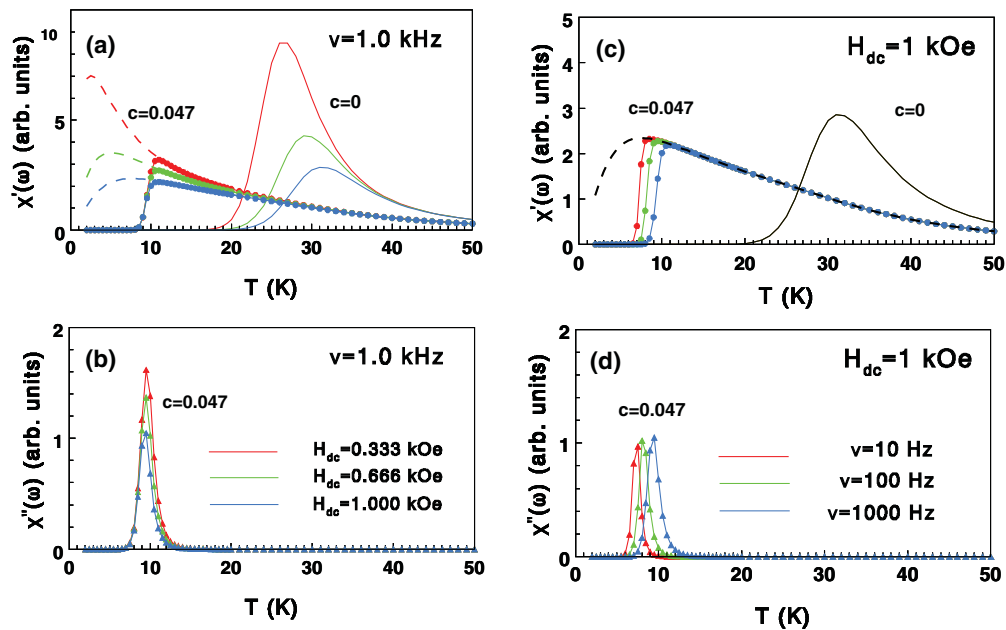


FIG. 7. (Color online) Temperature dependence of the dynamic susceptibility of CoPhOMe, calculated for a doped chain ($c = 0.047$) in the single-frequency approximation [Eq. (33)], for the same values of frequency and dc field as in Fig. 6. Thin dashed lines denote the static susceptibility of the doped system ($c = 0.047$) versus T . Thin solid lines denote the dynamic susceptibility of the infinite chain ($c = 0$): notice the absence of any frequency dependence for fixed $H_{dc} = 1$ kOe [see (c)] at the chosen values of ν .

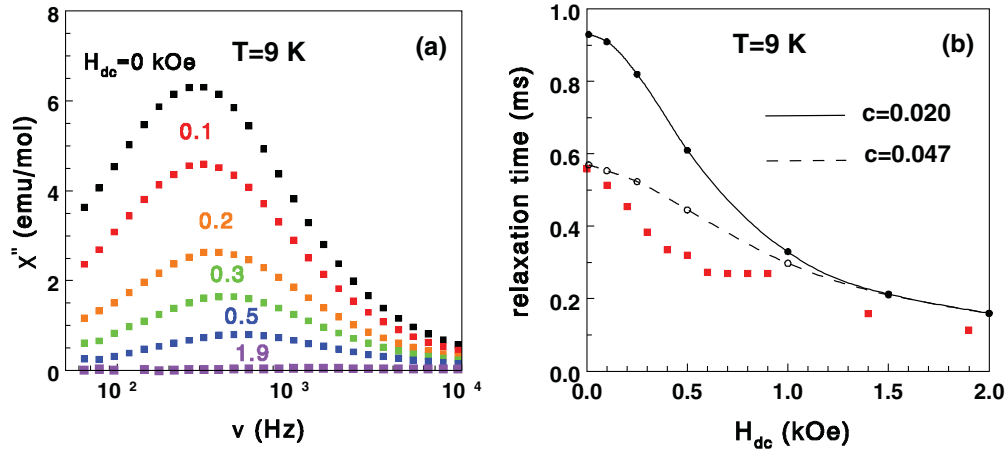


FIG. 8. (Color online) (a) Frequency dependence of the imaginary part of the ac susceptibility, χ'' , measured in CoPhOMe at fixed temperature $T = 9$ K for selected values of the static magnetic field. (b) Field dependence of the relaxation time τ of the magnetization of CoPhOMe as deduced from the peak position of χ'' versus frequency at $T = 9$ K. Squares denote experimental results; the lines connect theoretical values calculated for a doped chain in the approximation of a single dominating frequency for each segment length [Eq. (33)], using $J_I/k_B = 80$ K, $g = 2$, and $\tau_0 = 4 \times 10^{-13}$ s.

$H_{dc} = 25$ kOe, the field was swept to a new H_{dc} value with a field sweep rate of about 250 Oe/s, and the time dependence of the magnetization of the system was recorded in the presence of an applied static magnetic field. The relaxation of the magnetization as a function of time in nonzero field, measured using a Cryogenic S600 SQUID magnetometer, is reported in Fig. 9(a). The magnetization was fitted using a monoexponential law, $M(t) = M(t_0) + a_1 e^{-(t-t_0)/\tau}$, and we obtained the relaxation time τ versus H reported (red squares) in Fig. 9(b).

In both cases, the experimental relaxation time presents a maximum for $H_{dc} = 0$, but the low-field behavior is rather different: ac data at higher temperature ($T = 9$ K) present a smooth dependence, while dc data at lower temperature ($T = 5.1$ K) display a sharp maximum.

For an infinite Ising chain or for an open chain segment of fixed length L (expressed in lattice units), the dependence of the normalized frequency (i.e., inverse of relaxation time) on the static field in the critical regime ($e^{2K}h \ll 1$ or $Lh \ll$

1, respectively) is expected to be quadratic:²⁹ $\nu_{\text{nor}}(h_0) = \tau(h_0 = 0)/\tau(h_0) = 1 + (a_i h_0)^2$, where $a_i \propto e^{2K}$ or $a_i \propto L$, respectively. In Fig. 10 we show that the relaxation data for CoPhOMe, obtained from ac measurements at $T = 9$ K and from dc measurements at $T = 5.1$ K, indeed display a quadratic dependence on h_0 at very low fields, thus confirming the correctness of the Ising model. From data fitting (dashed curves in Fig. 10) one can deduce an order of magnitude for a_i and, according to the relationship $a_i \approx 0.82L$, valid for $L \ll e^{2K}$,²⁹ an estimate for an effective mean chain length \bar{L} . From dc data at $T = 5.1$ K one obtains $\bar{L} \approx 548$, while from ac data at $T = 9$ K the estimated mean chain length is $\bar{L} \approx 172$. The higher value obtained for \bar{L} in the former case is consistent with the higher quality of the single-crystal sample used for the dc measurements.

Considering that even nominally pure samples are strongly nonhomogeneous, a data analysis in terms of a single effective \bar{L} seems too rough. For the interpretation of the τ versus H experiments, we thus assumed concentrations of

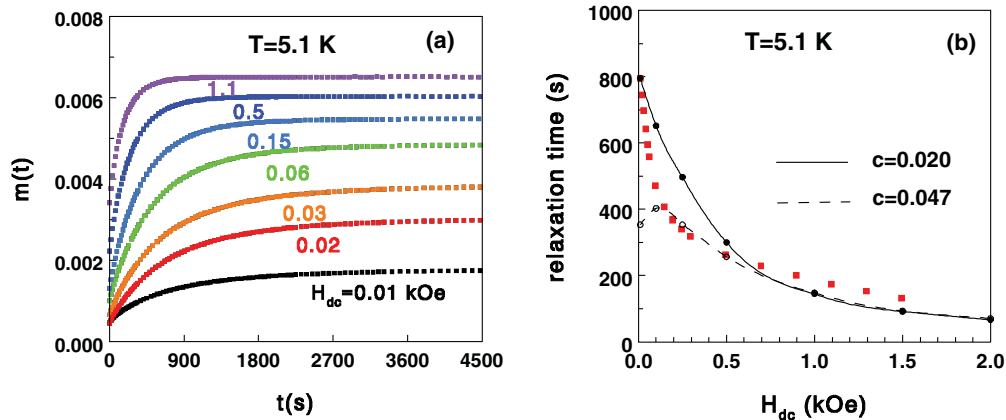


FIG. 9. (Color online) (a) Time dependence of the magnetization $m(t)$, measured in CoPhOMe at fixed temperature $T = 5.1$ K for selected values of the static magnetic field. (b) Field dependence of the relaxation time τ of the magnetization of CoPhOMe. Squares denote experimental results obtained by an exponential fit of $m(t)$; the line connects theoretical values determined as in Fig. 7(b), but for $T = 5.1$ K.

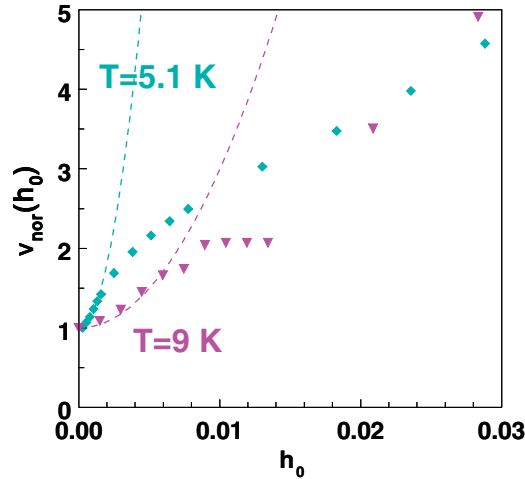


FIG. 10. (Color online) Normalized frequency $v_{\text{nor}}(h_0) = \tau(h_0 = 0)/\tau(h_0)$ versus reduced field $h_0 = g\mu_B H_{\text{dc}}/k_B T$, as deduced for CoPhOMe from ac data at $T = 9$ K (triangles) and dc data at $T = 5.1$ K (diamonds). The dashed lines denote a quadratic fit in h_0 : $v_{\text{nor}}(h_0) = 1 + (a_i h_0)^2$, where $a_i = 141.1$ from data at $T = 9$ K and $a_i = 449.7$ from data at $T = 5.1$ K.

randomly distributed, nonmagnetic impurities in the range $c \approx 0.02$ – 0.05 (i.e., comparable with those evidenced by dc and ac susceptibility measurements in the same compound: see Secs. III and V A, respectively). The theoretical curves for τ versus H , reported as full ($c = 0.02$) and dashed ($c = 0.047$) lines in Figs. 8(b) and 9(b), were determined as follows. First, the dynamic susceptibility $\chi(\omega)$ was calculated in the approximation of a single dominating frequency for each chain segment of N spins, opportunely weighted according to its static susceptibility and its probability of occurrence [see Eq. (33)]. Next, the frequency maximum of $\chi'(\omega)$ was taken to determine $\tau = 1/(\omega_{\text{max}})$. In order to reproduce the correct order of magnitude for the relaxation time τ of the magnetization of CoPhOMe (at both $T = 5.1$ and 9 K), one has to assume a value $\tau_0 \approx 4 \times 10^{-13}$ s for the characteristic time of spin flip of an isolated spin (the only free parameter in Glauber’s theory²). For the sake of simplicity, the same field-independent value was assumed in all calculations throughout the paper.

As regards the dc field dependence of the relaxation time of the magnetization, τ , we can conclude that it is qualitatively reproduced by theory, provided that finite-size effects are included. In fact, in a measurement performed for an inhomogeneous CoPhOMe sample, no appreciable contribution to the relaxation time τ is expected from the infinite chain at low temperatures, owing to the high value of the exchange coupling ($J_1/k_B = 80$ K). For example, from Eq. (17), putting $\tau_0 = 4 \times 10^{-13}$ s, at $T = 5$ K one has $\tau_\infty = 1.25 \times 10^{15}$ s for $H_{\text{dc}} = 0$, while in a static field $H_{\text{dc}} = 10$ Oe the relaxation time reduces to $\tau_\infty = 2.77 \times 10^{-6}$ s. In contrast, an experimentally appreciable relaxation time is associated with finite-size chains. To achieve a quantitative agreement, as regards the field dependence of τ , further work is required. This quite interesting task, however, is deferred to the future. In fact, our primary concern in the present paper was the study of the frequency-dependent magnetic susceptibility, representing

the response function of the system to an oscillating magnetic field.²

VI. CONCLUSIONS

In this paper, the spin dynamics of the archetypal molecular magnetic chain CoPhOMe in the presence of an external magnetic field of any intensity was investigated using a simplified model, consisting of a one-dimensional Ising ferromagnet with a stochastic dynamics caused by the interaction of the spins with a heat reservoir.²

In the framework of a local-equilibrium approximation, devised to truncate the infinite sequence of kinetic equations originated by the presence of a nonzero static magnetic field, and of a linear response of the system to a small oscillating field, we first calculated the dynamic susceptibility of an infinite chain. Next, the theory was generalized to a finite, open Ising chain. We showed that the dynamic susceptibility of an open chain with a finite number N of spins can be expressed as a weighted sum of N frequency contributions, related to the N relaxation rates of the magnetization fluctuations. From the comparison with the ac susceptibility data obtained for nominally pure samples we can draw two conclusions: (i) the pure samples are really nonhomogeneous, because regions with very low density of defects coexist with regions with a relevant density of defects; (ii) only the latter regions show a contribution to the dynamic relaxation, in the frequency range conventionally investigated by ac susceptibility measurements.

For doped CoPhOMe chains, the approximation of a single dominating frequency for each segment length was found to be quite satisfactory in order to account for ac susceptibility data²⁶ in a moderate static magnetic field ($H_{\text{dc}} = 2$ kOe), as a function both of temperature and of the frequency of the small oscillating field.

Finally, it is worth observing that, on the basis of our calculation of the T and H dependence of the relaxation rates (and corresponding frequency weights), we do not expect that the approximation of a single dominating frequency for each segment length will be able to account for ¹H nuclear magnetic resonance and muon spin rotation experimental data^{37,38,40,41} in pure and zinc-doped CoPhOMe, because these techniques probe the local spin dynamics at frequencies ($\nu \approx$ MHz) substantially higher than the typical frequencies ($\nu \approx$ kHz) used in an ac susceptibility experiment. Anyway, the present results constitute a fundamental background for the future theoretical investigation of such high-frequency regimes.

ACKNOWLEDGMENTS

Fruitful discussions with P. Santini and P. Politi are gratefully acknowledged. Financial support was provided by MIUR (Italian Ministry for University and Research) under the PRIN Program (Contract No. 2008PARRTS 003) entitled “Topological Effects and Entanglement in Molecular Chains and Clusters of Spins.” L.B. acknowledges financial support from the German Ministry of Science via DFG, SFB-TRR21, and the Sofja Kovalevskaja grant from the Humboldt Stiftung.

APPENDIX: RELAXATION TIMES OF AN OPEN CHAIN OF N ISING SPINS IN AN APPLIED MAGNETIC FIELD

In order to calculate the relaxation times of an open chain of N spins coupled by the Ising exchange Hamiltonian and subject to a static magnetic field H , Eq. (4), following Glauber² one starts by writing the kinetic equation of motion for the time-dependent average of an interior spin ($\langle\sigma_p\rangle$) with $1 < p < N$,

$$\tau_0 \frac{d\langle\sigma_p\rangle}{dt} = -\langle\sigma_p\rangle + \frac{\gamma}{2} [\langle\sigma_{p-1}\rangle + \langle\sigma_{p+1}\rangle] + \tanh h(t) \times \left[1 - \frac{\gamma}{2} (\langle\sigma_{p-1}\sigma_p\rangle + \langle\sigma_p\sigma_{p+1}\rangle) \right], \quad (\text{A1})$$

where τ_0 is the characteristic time for the spin flip of an isolated spin, $\gamma = \tanh(2K)$, and $h(t) = \frac{g\mu_B H(t)}{k_B T}$. For the two spins ($p = 1$ and $p = N$) located at the ends of the open chain, following Coulon *et al.*,²⁹ one has instead

$$\tau_0 \frac{d\langle\sigma_1\rangle}{dt} = -\langle\sigma_1\rangle + \eta\langle\sigma_2\rangle + \tanh h(t)[1 - \eta\langle\sigma_1\sigma_2\rangle], \quad (\text{A2})$$

$$\tau_0 \frac{d\langle\sigma_N\rangle}{dt} = -\langle\sigma_N\rangle + \eta\langle\sigma_{N-1}\rangle + \tanh h(t)[1 - \eta\langle\sigma_{N-1}\sigma_N\rangle], \quad (\text{A3})$$

where $\eta = \tanh K$.² In our case [see Eq. (10)], the time-dependent magnetic field is assumed to be $H(t) = H_{\text{dc}} + H_1 e^{-i\omega t}$, i.e., the sum of a static dc field of any intensity, H_{dc} , and of a much lower ac field, $H_1 \ll H_{\text{dc}}$, oscillating at the angular frequency ω . Thus we can expand $\tanh h(t) \approx \tanh h_0 + h_1 e^{-i\omega t} (1 - \tanh^2 h_0)$, where $h_0 = \frac{g\mu_B H_{\text{dc}}}{k_B T}$ and $h_1 = \frac{g\mu_B H_1}{k_B T}$.

Following Coulon *et al.*,²⁹ a linearization of Eqs. (A1), (A2), and (A3) around the spin equilibrium values is next performed in the framework of linear response theory (i.e., small departures from thermal equilibrium are assumed),

$$\langle\sigma_p\rangle \approx \langle\sigma_p\rangle_{N,\text{eq}} + \delta\langle\sigma_p\rangle, \quad (\text{A4})$$

$$\langle\sigma_p\sigma_{p+1}\rangle \approx \langle\sigma_p\sigma_{p+1}\rangle_{N,\text{eq}} + \delta\langle\sigma_p\sigma_{p+1}\rangle.$$

In this way, we obtain a system of N differential equations in the spin fluctuations ($\delta\langle\sigma_p\rangle$) with $p = 1, \dots, N$ where, on the right-hand sides, the presence of the field involves the presence of variations of time-dependent nearest-neighbor spin-spin correlation functions ($\delta\langle\sigma_p\sigma_{p+1}\rangle$),

$$\begin{aligned} \tau_0 \frac{d\delta\langle\sigma_1\rangle}{dt} &= -\delta\langle\sigma_1\rangle + \eta[\delta\langle\sigma_2\rangle - \tanh h_0 \delta\langle\sigma_1\sigma_2\rangle] + h_1 e^{-i\omega t} (1 - \tanh^2 h_0) [1 - \eta\langle\sigma_1\sigma_2\rangle_{N,\text{eq}}], \\ \tau_0 \frac{d\delta\langle\sigma_p\rangle}{dt} &= -\delta\langle\sigma_p\rangle + \frac{\gamma}{2} [\delta\langle\sigma_{p-1}\rangle + \delta\langle\sigma_{p+1}\rangle] - \tanh h_0 (\delta\langle\sigma_{p-1}\sigma_p\rangle + \delta\langle\sigma_p\sigma_{p+1}\rangle) \\ &\quad + h_1 e^{-i\omega t} (1 - \tanh^2 h_0) \left[1 - \frac{\gamma}{2} (\langle\sigma_{p-1}\sigma_p\rangle_{N,\text{eq}} + \langle\sigma_p\sigma_{p+1}\rangle_{N,\text{eq}}) \right], \\ \tau_0 \frac{d\delta\langle\sigma_N\rangle}{dt} &= -\delta\langle\sigma_N\rangle + \eta[\delta\langle\sigma_{N-1}\rangle - \tanh h_0 \delta\langle\sigma_{N-1}\sigma_N\rangle] + h_1 e^{-i\omega t} (1 - \tanh^2 h_0) [1 - \eta\langle\sigma_{N-1}\sigma_N\rangle_{N,\text{eq}}]. \end{aligned} \quad (\text{A5})$$

If one writes down the kinetic equations for $\delta\langle\sigma_p\sigma_{p+1}\rangle$, one finds an infinite sequence of equations involving other, higher-order spin correlation functions. Such an infinite hierarchy of equations can be decoupled by resorting to the local-equilibrium approximation first proposed by Huang in the case of the kinetic equation of an infinite Ising chain in a magnetic field:³⁰ i.e., the relation existing between the magnetization and the correlation function at thermal equilibrium⁴² is assumed to hold *locally* although the system is not in equilibrium ($t \neq 0$). The advantage of the local-equilibrium approximation with respect to perturbative methods² or the mean-field approximation is that it provides an exact steady-state solution.³⁰

In the case of a finite chain with N spins, the local-equilibrium approximation was implemented, following Coulon *et al.*,²⁹ by expressing the variations of two-spin correlation functions in terms of a linear combination of the variations of single-spin averages,

$$\delta\langle\sigma_p\sigma_{p+1}\rangle = A_{N,p} \delta\langle\sigma_p\rangle + B_{N,p} \delta\langle\sigma_{p+1}\rangle. \quad (\text{A6})$$

The coefficients are²⁹

$$\begin{aligned} A_{N,p} &= \frac{\langle\sigma_{N-p}\rangle_{N-p,\text{eq}} - \eta\langle\sigma_p\rangle_{p,\text{eq}}}{1 - \eta\langle\sigma_p\rangle_{p,\text{eq}}\langle\sigma_{N-p}\rangle_{N-p,\text{eq}}}, \\ B_{N,p} &= \frac{\langle\sigma_p\rangle_{p,\text{eq}} - \eta\langle\sigma_{N-p}\rangle_{N-p,\text{eq}}}{1 - \eta\langle\sigma_p\rangle_{p,\text{eq}}\langle\sigma_{N-p}\rangle_{N-p,\text{eq}}}, \end{aligned} \quad (\text{A7})$$

where the average spin values can be calculated, at thermal equilibrium, by using the recursive relation⁵⁰

$$\langle\sigma_p\rangle_{p,\text{eq}} = \frac{\tanh h_0 + \eta\langle\sigma_{p-1}\rangle_{p-1,\text{eq}}}{1 + \eta \tanh h_0 \langle\sigma_{p-1}\rangle_{p-1,\text{eq}}} \quad (\text{A8})$$

with the initial condition $\langle\sigma_1\rangle_{1,\text{eq}} = \tanh h_0$. The set of N linear differential equations in the N variables $\delta\langle\sigma_p\rangle$ can be rewritten in matrix form as

$$\tau_0 \frac{d\mathbf{\Sigma}}{dt} = -\mathbf{Y} \cdot \mathbf{\Sigma} + h_1 e^{-i\omega t} (1 - \tanh^2 h_0) \mathbf{\Psi}. \quad (\text{A9})$$

The $N \times 1$ vector $\mathbf{\Sigma}$ has elements $\Sigma_p = \delta\langle\sigma_p\rangle$ ($p = 1, \dots, N$). \mathbf{Y} is a real, symmetric, tridiagonal $N \times N$ matrix whose

nonzero elements are ($1 < p < N$)

$$\begin{aligned}
 Y_{1,1} &= 1 + \eta A_{N,1} \tanh h_0, & Y_{1,2} &= \eta(B_{N,1} \tanh h_0 - 1), \\
 Y_{p-1,p} &= \frac{\gamma}{2}(A_{N,p-1} \tanh h_0 - 1), & Y_{p,p} &= 1 + \frac{\gamma}{2}(A_{N,p} + B_{N,p-1}) \tanh h_0, & Y_{p,p+1} &= \frac{\gamma}{2}(B_{N,p} \tanh h_0 - 1), \\
 Y_{N,N-1} &= \eta(A_{N,N-1} \tanh h_0 - 1), & Y_{N,N} &= 1 + \eta B_{N,N-1} \tanh h_0.
 \end{aligned} \tag{A10}$$

The $N \times 1$ vector Ψ in Eq. (A9) has elements

$$\begin{aligned}
 \Psi_1 &= 1 - \eta \langle \sigma_1 \sigma_2 \rangle_{N,\text{eq}}, \\
 \Psi_p &= 1 - \frac{\gamma}{2} [\langle \sigma_{p-1} \sigma_p \rangle_{N,\text{eq}} + \langle \sigma_p \sigma_{p+1} \rangle_{N,\text{eq}}], & 1 < p < N, \\
 \Psi_N &= 1 - \eta \langle \sigma_{N-1} \sigma_N \rangle_{N,\text{eq}} = \Psi_1.
 \end{aligned} \tag{A11}$$

Equation (A9) can be solved, e.g., using the method of eigenfunctions.^{44,45} As shown in Sec. IV B, the N eigenvalues of \mathbf{Y} are related to the N frequencies (28) of the finite, open Ising chain of N spins, while the N eigenfunctions are required in order to calculate the corresponding frequency weights (29), involved in the expression of the dynamic susceptibility (27).

- ¹J. Villain, *Physica B+C* **79**, 1 (1975).
²R. J. Glauber, *J. Math. Phys.* **4**, 294 (1963).
³R. J. Baxter, *Exactly Solved Models in Statistical Mechanics* (Dover, Mineola, NY, 2007).
⁴R. Cordery, S. Sarker, and J. Tobochnik, *Phys. Rev. B* **24**, 5402 (1981).
⁵B. Khoushnevisan and S. Beheshti, Iran. Journ. Crystall. Mineral. **16**, 646 (2009).
⁶E. Scheidman, M. J. Berry, R. Segev, and W. Bialek, *Nature (London)* **440**, 1007 (2006).
⁷J. L. Skinner, *J. Chem. Phys.* **79**, 1955 (1983).
⁸D. Stauffer, *J. Math. Sociol.* **28**, 25 (2004).
⁹D. Stauffer, *Eur. J. Phys.* **26**, 579 (2005).
¹⁰A. Caneschi, D. Gatteschi, N. Lalioti, C. Sangregorio, R. Sessoli, G. Venturi, A. Vindigni, A. Rettori, and M. G. Pini, *Angew. Chem., Int. Ed.* **40**, 1760 (2001).
¹¹A. Vindigni, A. Rettori, L. Bogani, A. Caneschi, D. Gatteschi, R. Sessoli, and M. A. Novak, *Appl. Phys. Lett.* **87**, 073102 (2005).
¹²W. Wernsdorfer, R. Clerac, C. Coulon, L. Lecren, and H. Miyasaka, *Phys. Rev. Lett.* **95**, 237203 (2005).
¹³C. Coulon, H. Miyasaka, and R. Clérac, *Struct. Bonding (Berlin)* **122**, 163 (2006).
¹⁴L. Bogani, A. Vindigni, R. Sessoli, and D. Gatteschi, *J. Mater. Chem.* **18**, 4750 (2008).
¹⁵D. Gatteschi, L. Bogani, A. Cornia, M. Mannini, L. Sorace, and R. Sessoli, *Solid State Sci.* **10**, 1701 (2008).
¹⁶R. Lescouezec, J. Vaissermann, C. Ruiz-Perez, F. Lloret, R. Carrasco, M. Julve, M. Verdaguer, Y. Dromzee, D. Gatteschi, and W. Wernsdorfer, *Angew. Chem., Int. Ed.* **42**, 1483 (2003).
¹⁷T. F. Liu, D. Fu, S. Gao, Y. Z. Zhang, H. L. Sun, G. Su, and Y. J. Liu, *J. Am. Chem. Soc.* **125**, 13976 (2003).
¹⁸L. Bogani, C. Sangregorio, R. Sessoli, and D. Gatteschi, *Angew. Chem., Int. Ed.* **44**, 5817 (2005).
¹⁹M. Ferbinteanu, H. Miyasaka, W. Wernsdorfer, K. Nakata, K. Sugiura, M. Yamashita, C. Coulon, and R. Clerac, *J. Am. Chem. Soc.* **127**, 3090 (2005).
²⁰T. Kajiwara, M. Nakano, Y. Kaneko, S. Takaishi, T. Ito, M. Yamashita, A. Igashira-Kamiyama, H. Nojiri, Y. Ono, and N. Kojima, *J. Am. Chem. Soc.* **127**, 10150 (2005).
²¹J. K. L. da Silva, A. G. Moreira, M. S. Soares, and F. C. Sá Barreto, *Phys. Rev. E* **52**, 4527 (1995).
²²J. H. Luscombe, M. Luban, and J. P. Reynolds, *Phys. Rev. E* **53**, 5852 (1996).
²³A. Caneschi, D. Gatteschi, N. Lalioti, C. Sangregorio, R. Sessoli, G. Venturi, A. Vindigni, A. Rettori, M. G. Pini, and M. A. Novak, *Europhys. Lett.* **58**, 771 (2002).
²⁴L. Bogani, A. Caneschi, M. Fedi, D. Gatteschi, M. Massi, M. A. Novak, M. G. Pini, A. Rettori, R. Sessoli, and A. Vindigni, *Phys. Rev. Lett.* **92**, 207204 (2004).
²⁵A. Vindigni, L. Bogani, D. Gatteschi, R. Sessoli, A. Rettori, and M. A. Novak, *J. Magn. Magn. Mater.* **272-276**, 297 (2004).
²⁶L. Bogani, R. Sessoli, M. G. Pini, A. Rettori, M. A. Novak, P. Rosa, M. Massi, M. E. Fedi, L. Giuntini, A. Caneschi *et al.*, *Phys. Rev. B* **72**, 064406 (2005).
²⁷X. J. Li, X. Y. Wang, S. Gao, and R. Gao, *Inorg. Chem.* **45**, 1508 (2006).
²⁸A. Baumgärtner and K. Binder, *J. Stat. Phys.* **18**, 423 (1978).
²⁹C. Coulon, R. Clérac, W. Wernsdorfer, T. Colin, A. Saitoh, N. Motokawa, and H. Miyasaka, *Phys. Rev. B* **76**, 214422 (2007).
³⁰H. W. Huang, *Phys. Rev. A* **8**, 2553 (1973).
³¹A. Caneschi, D. Gatteschi, N. Lalioti, L. Sorace, R. Sessoli, V. Tangoulis, and A. Vindigni, *Chem. Eur. J.* **8**, 286 (2002).
³²A. Vindigni and M. G. Pini, *J. Phys.: Condens. Matter* **21**, 236007 (2009).
³³C. Coulon, R. Clérac, L. Lecren, W. Wernsdorfer, and H. Miyasaka, *Phys. Rev. B* **69**, 132408 (2004).
³⁴B. Barbara, *J. Magn. Magn. Mater.* **129**, 79 (1994).
³⁵M. Balandia, M. Rams, S. K. Nayak, Z. Tomkowicz, W. Haase, K. Tomala, and J. V. Yakhmi, *Phys. Rev. B* **74**, 224421 (2006).
³⁶O. V. Billoni, V. Pianet, D. Pescia, and A. Vindigni, *Phys. Rev. B* **84**, 064415 (2011).
³⁷A. Lascialfari, E. Micotti, S. Aldovrandi, A. Caneschi, and D. Gatteschi, *J. Appl. Phys.* **93**, 8749 (2003).
³⁸M. Mariani, S. Aldovrandi, M. Corti, A. Lascialfari, L. Bogani, A. Caneschi, and R. Sessoli, *Inorg. Chim. Acta* **361**, 4107 (2008).
³⁹M. Wortis, *Phys. Rev. B* **10**, 4665 (1974).

- ⁴⁰E. Micotti, A. Lascialfari, A. Rigamonti, S. Aldovrandi, A. Caneschi, D. Gatteschi, and L. Bogani, *J. Magn. Magn. Mater.* **272-276**, 1087 (2004).
- ⁴¹M. Mariani, S. Aldovrandi, M. Corti, J. Lago, A. Lascialfari, E. Micotti, A. Rettori, F. Cinti, A. Amato, C. Baines *et al.*, *Inorg. Chim. Acta* **360**, 3903 (2007).
- ⁴²J. S. Marsh, *Phys. Rev.* **145**, 251 (1966).
- ⁴³J. J. Brey and A. Prados, *Phys. Lett. A* **216**, 240 (1996).
- ⁴⁴N. G. van Kampen, *Stochastic Processes in Physics and Chemistry* (North-Holland, Amsterdam, 1981).
- ⁴⁵J. J. Brey and A. Prados, *Phys. Rev. E* **53**, 458 (1996).
- ⁴⁶P. Santini, S. Carretta, E. Livioti, G. Amoretti, P. Carretta, M. Filibian, A. Lascialfari, and E. Micotti, *Phys. Rev. Lett.* **94**, 077203 (2005).
- ⁴⁷A. Bianchi, S. Carretta, P. Santini, G. Amoretti, J. Lago, M. Corti, A. Lascialfari, P. Arosio, G. Timco, and R. E. P. Winpenny, *Phys. Rev. B* **82**, 134403 (2010).
- ⁴⁸M. G. Pini and A. Rettori, *Phys. Rev. B* **76**, 064407 (2007).
- ⁴⁹D. Gatteschi, R. Sessoli, and J. Villain, *Molecular Nanomagnets* (Oxford University Press, New York, 2006).
- ⁵⁰F. Matsubara, K. Yoshimura, and S. Katsura, *Can. J. Phys.* **51**, 1053 (1973).